International Research Journal of Engineering and Technology (IRJET) e-ISSN: 2395-0056
Volume: 11 Issue: 09 | Sep 2024 www.irjet.net p-ISSN: 2395-0072

DESIGN AND IMPLEMENTATION OF H-BRIDGE MULTILEVEL INVERTER FOR GRID INTEGRATION

R RAKSHITH[1], Dr. HEMALATHA J N[2], Dr. MADHU B R[3]

[1]Student, EEE Dept., RV College of Engineering, Bengaluru, India
[2] Associate Professor, EEE Dept., RV College of Engineering, Bengaluru, India
[3] Assistant Professor, EEE Dept., RV College of Engineering, Bengaluru, India

---

Abstract - ***This paper work is aimed at design and simulation analysis of two-stage grid connected photovoltaic(PV) system using SEPIC converter and modified H-Bridge multilevel inverter. The first stage has a Coupled Inductor based Single Ended Primary Inductor Converter(SEPIC) with Incremental Conductance Maximum Power Point Tracking(MPPT) algorithm that aid in tracking the Maximum Power Point of the PV system with high tracking speed and output efficiency. The second stage is a modified three phase H-Bridge Multilevel Inverter controlled by second order generalized integral (SOGI) technique for pumping the sinusoidal and less distorted power extracted from PV into the distribution grid. The modeling of proposed system was carried out on the PV module of total capacity of 2100W to obtain improved efficient power extraction.***

***Key Words*: SEPIC Converter, DC-DC Converter, DC-AC Converter, H-Bridge Multilevel Inverter, Maximum Power Point Tracking, Total harmonic distortion, Photo Voltaic, Matlab, Simulink**

1. INTRODUCTION

In recent days the use of renewable energy is widely increasing day by day. Among them, Solar Energy is considered as one of the important energy sources since these are environmental friendly and produces electric power without causing pollution. Therefore, Solar Photo Voltaic (PV) panels are preferred that are readily available. The PV system is stationary, silent, free of mechanical parts, and has low running and manufacturing costs compared to other renewable resources. The use of photovoltaic as a source of electrical energy shows a growing trend both in the implementation of the global sector and in the performance of various industrial plants. This trend is motivated by many factors, such as decrease in the cost of producing photovoltaic electricity per kW and the rise in fossil fuel prices and the development of effective photovoltaic energy conversion technology [1-4].

The photovoltaic cells generate electrical energy using the sunlight. A PV panel is formed of PV cells connected in series, parallel or series-parallel that is working commonly with a DC-DC converter and stores electrical energy in a battery array. In other situations, a DC-AC inverter is used to connect the PV panel and DC-DC converter in order to add electricity to the grid. When it comes to inverters, multilevel inverters (MLIs) and two level inverters are typically utilized [5]. Comparing MLI to two-level inverters, the former is more appealing due to lower switching stresses, lower operating frequency, and smaller filter requirements. There have been reports of several enhanced topologies with smaller filters, more stages, less Total Harmonic Distortion (THD), and fewer switches. In this operation, the DC-DC converter must run at its Maximum Power Point (MPP) in order to increase the generating efficiency. Therefore, tracking this point requires an algorithm. The MPPT algorithm is applied to find the maximum point that adjusts the duty cycle of the converter to increase the generation efficiency [8].

Generally , the system that are connected to the grid are of two stages, the first stage is DC-to-DC converters that boosts the PV voltages and extract the Maximum Power by utilizing MPPT and the stage two is to invert this DC power to AC power. The Maximum Power Point Tracking (MPPT) algorithm is used to track the maximum power the solar array. The second order generalized integral (SOGI) technique is used to control the multilevel inverter. In the proposed system it reduces complexity, less weight, low cost, high efficiency, and sinusoidal current is injected into the grid [7].

2. CIRCUIT SCHEME

Figure 1 depicts the methodology of the proposed system. It consists of dual-stage conversion: a DC-DC conversion stage and a DC-AC conversion stage. DC-DC converter ie., Single Input Multiple Output SEPIC Converter, consists of an active switch (S_m), two diodes (D_1, D_2), input inductor and capacitor (C_b, L_m) coupled to two split capacitors (C_1 *and* C_2), connected to a DC link. The input to the SIMO-SEPIC Converter is given from the PV panel that generates DC current from the sun's rays. The SEPIC Converter regulates and boosts up the DC output voltage to suitable levels and feeds it to the proposed H-Bridge Multilevel Inverter. The SIMO-SEPIC Converter is controlled by Incremental Conductance MPPT Algorithm.

The modified H-Bridge multilevel inverter consists of 6 active switches (S_1, S_2, S_3, S_4, S_5, S_6), the input to the inverter is given from the SEPIC Converter, here the multilevel inverter converts DC to 5-Level AC. The switches of the

multilevel inverter is controlled and regulated by second order generalised integral (SOGI) technique using PLL technique. The output of the multilevel inverter is fed to the load and the distribution grid.

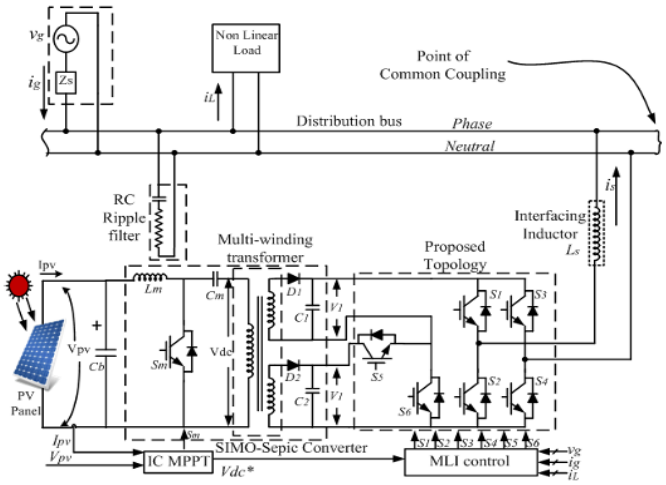

Figure 1: Circuit Scheme of the Proposed System

3. MODE OF OPERATION OF H- BRIDGE MULTILEVEL INVERTER

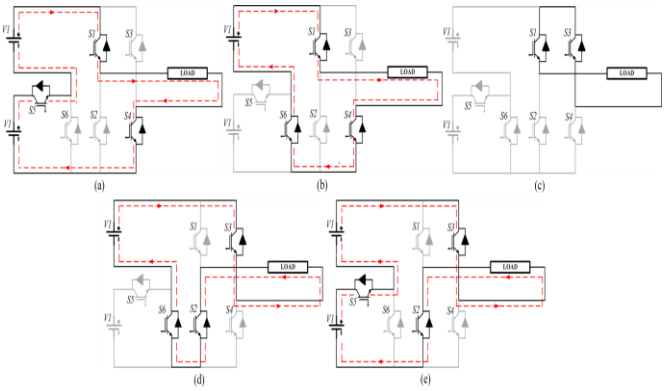

Figure 2: Mode of Operation

Mode of operation of H-Bridge Multilevel Inverter is explained below:

Table 2.2, shows the switching states for different voltage levels.

MODE 1- Switches S_1, S_4 and S_5 are turned ON. The output voltage value is $2V_1$. The switches S_2, S_3, S_6 are off. The equivalent circuit is shown in Figure 2 (a).

MODE 2- Switches S_1, S_4 and S_6 are turned ON. The output voltage value is V1. The switches S_2, S_3, S_5 are off. The equivalent circuit is shown in Figure2 (b).

MODE 3- Switches S_1 and S_3 are turned ON. The output voltage value is zero. The switches S_2, S_4,S_5, S_6 are off. The equivalent circuit is shown Figure 2 (c).

MODE 4- Switches S_2, S_3 *and* S_6 are turned ON. The output voltage value is −V1. The switches S_1, S_4,S_5 are off. The equivalent circuit is shown in Figure 2 (d).

MODE 5- Switches S_2 , S_3 and S_5 are turned ON. The output voltage value is $-2V_1$. The switches S_1, S_4, S_6 are off. The equivalent circuit is shown in Figure 2 (e).

Table 1: Switching States for Different Voltage Levels

Voltage Level	S_1	S_2	S_3	S_4	S_5	S_6
$+2V_1$	1	0	0	1	1	0
$+V_1$	1	0	0	1	0	1
0	1	0	1	0	0	0
$-V_1$	0	1	1	0	0	1
$-2V_1$	0	1	1	0	1	0

4. INCREMENTAL CONDUCTANCE MPPT TECHNIQUE

The INC MPPT approach is based on the fact that, the slope of the P-V curve is zero at the MPP, positive to the left of the MPP, and negative to the right of the MPP. INC conditions that are expressed in Equations.1, 2, 3.

$$\frac{dP}{dV} = 0 \quad at\ MPP \tag{1}$$

$$\frac{dP}{dV} > 0 \quad Left\ to\ MPP \tag{2}$$

$$\frac{dP}{dV} < 0 \quad Right\ to\ MPP \tag{3}$$

The INC MPPT method has the advantage of being able to compute and determine the exact perturbation direction for the operating voltage of PV modules that is superior to the other two HC and P&O algorithms.

If the MPP is determined using the INC method's judgment conditions (dI/dV = I/V and dI = 0), it can theoretically prevent the perturbation phenomenon that occurs at the maximum power point that occur in the other MPPT logics. After that, the operating voltages are set. During experimental experiments, however, it appears that the perturbation phenomena are still occurring around the MPP under non-uniform weather circumstances. Because the likelihood of satisfying condition dI/dV = I/V is extremely low, and the deterministic process of the INC algorithm is more sophisticated, the simulation time spent on INC

algorithm is much longer than compared to HC and P&O methods.

The MPP is tracked by seeking the peak of the P-V curve using the incremental conductance technique that detects the slope of the P-V curve. The instantaneous conductance I/V and incremental conductance dI/dV are used in this MPPT algorithm. The location of the PV module's operating point in the P-V curve is determined based on the relationship between the two values, as expressed in equations 1,2,3, ie., (1) indicates the P module operates at the MPP, whereas (2) and (3) indicate the PV module operates on the left and right sides of the MPP in the P-V curve, respectively.

5. DESIGN OF SEPIC CONVERTER

The Table 2 gives the information about the input and output parameters required for the design of the Two Parallel Interleaved DC-DC Converter.

Table 2: Design Specifications

PV Array	Module	Apollo Solar Energy ASEC-300G6M (Polycrystalline Module)
	Series Connected Modules	7 No's
	Total Power Output	2100 W
	Voltage at MPP	249 V
	Short Circuit Current	8.45 A
DC-DC CONVERTER	Input Voltage	250 V
	Output Voltage	320 V
	Switching Frequency	100kHz
	Power	2 kW
	Output Current	6.25 A
H-BRIDGE MULTILEVEL INVERTER	Input Voltage	320 V
	Output Voltage	230 V
	Frequency	50 Hz

The SEPIC Converter delivers 320 V DC to the multilevel inverter using an input DC voltage of 250 Volts. Considering the given specifications for the converter shown in table 4.1.

The duty ratio, D is provided by the following relation (V_{FWD} = 0):

$$D = \frac{V_{OUT}+V_{FWD}}{V_{IN}+V_{OUT}+V_{FWD}} \quad (4)$$

Where, V_{OUT}= Output Voltage

V_{IN}= Input Voltage

V_{FWD}= Forward Diode Voltage

$$D = \frac{320}{250+320}$$

$$D = 0.56$$

The average of input side inductor current is provided in the following equation:

$$I_L = I_{OUT}\frac{V_{OUT}}{V_{IN}} \quad (5)$$

Where, I_{OUT}= Output Current

$$I_L = 6.25 \times \frac{320}{250}$$

$$I_L = 8A$$

The switching time period, T_s is calculated from the switching frequency as shown below:

$$T_S = \frac{1}{F_S} \quad (6)$$

Where, F_S= Switching Frequency

$$T_S = \frac{1}{100K}$$

$$T_S = 10\mu sec$$

The input side inductance is calculated from the equation below:

$$L_M = \frac{2(1-D)^2 R T_S}{D} \quad (7)$$

$$L_M = 0.36mH$$

The inductance value above calculated is termed as critical inductance. To ensure that the proposed converter operates in CCM under any load conditions, we must use larger inductors than that of calculated values.

The ripple inductor currents are taken as 20% of the actual inductor current values for both intermediate and input side inductances.

The intermediate inductance value can be calculated using the following equation:

$$L = (1 - D)RT_S \quad (8)$$

$$L = 0.224mH$$

The coupling capacitor is calculated from the following equation:

$$C_b = \frac{DT_S}{2.\frac{\Delta V_{Cb}}{V_{IN}}.R} \quad (9)$$

$$C_b = 6.15\mu F$$

The ripple voltage of coupling capacitor (ΔV_{cb}) is taken as 1% of the actual coupling capacitor voltage (V_{cb}).

The output capacitor is calculated from the following equation:

$$C_1, C_2 = \frac{\Delta I_{Cb}.T_S}{8\Delta V_{IN}} \quad (10)$$

$$C_1, C_2 = 2.4mF$$

The ripple voltage of output capacitor (ΔV_{co}) is taken as 1% of the actual output capacitor voltage (V_{co}).

Table 3: SEPIC Converter Design Parameters

SYMBOL	PARAMETERS	DESIGN VALUE
D	Duty Ratio	0.56
I_L	Input Inductor Current	8 A
T_S	Switching Time Period	10 µsec
L_M	Input Inductor	0.36 mH
L	Output Inductor	0.224 mH
C_b	Input Capacitor	6.15 µF
C_1, C_2	Output Capacitors	2.4 mF

6. SIMULATION RESULTS

The simulation circuit of H-bridge multi-level inverter for grid integration is shown in figure 3. A PV module of 250V, 2KW is connected to SEPIC converter integrated 5-level inverter in order to supply the load of 1KVA as well as grid of 50Hz. INC algorithm is used as MPPT in order to extract maximum power from PV module.

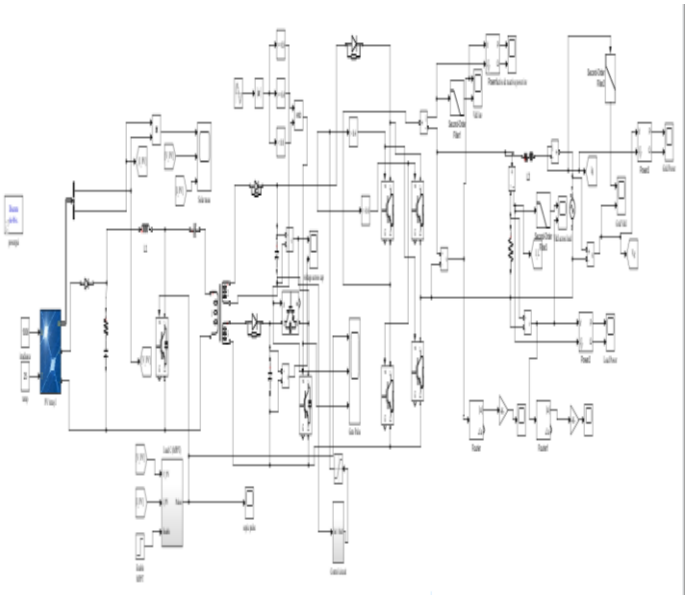

Fig3: Simulation Circuit

Figure 4, shows PV arrays power, voltage and current waveforms. The Power generated is around 2100W and the voltage and current is around 248.5 and 8.3 A respectively.

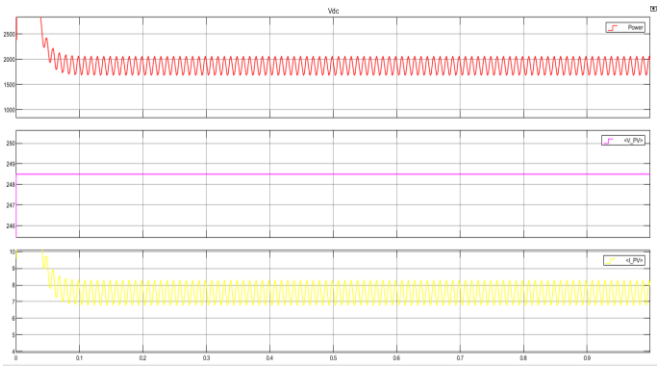

Figure 4: Power, Voltage, Current Waveforms of PV Array

Figure 5, shows the output-voltage and output-current waveforms of the H- Bridge Multilevel Inverter. The output voltage is around 300V and current is around 7A.

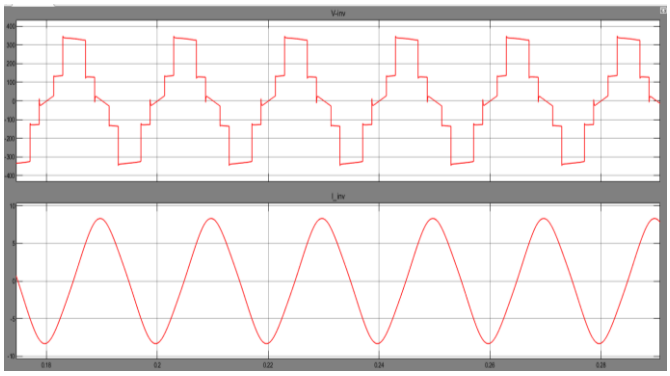

Figure 5: Inverter Voltage and Current Waveforms

The active power measured of the inverter is found to be around 1700W and the reactive power is around 0.7. Figure 6, shows the active and reactive power waveforms of inverter.

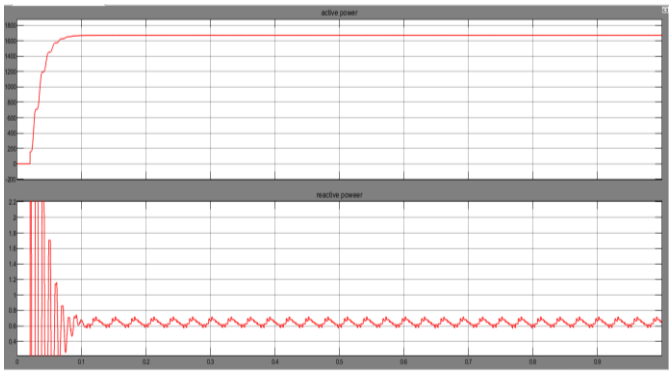

Figure 6: Inverter Power Waveforms

Figure 7, shows the current and voltage waveforms of the grid. Voltage o 230 Volts and current of 1.3A is observed from the waveforms.

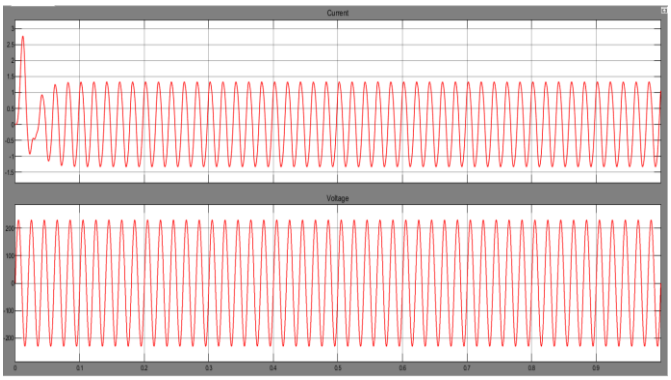

Figure 7: Grid Current and Voltage Waveforms

Figure 8, shows grids active and reactive power waveforms. The remaining power after being consumed by the load of 1KVA is being injected to the distribution grid, the active power is around 450VA.

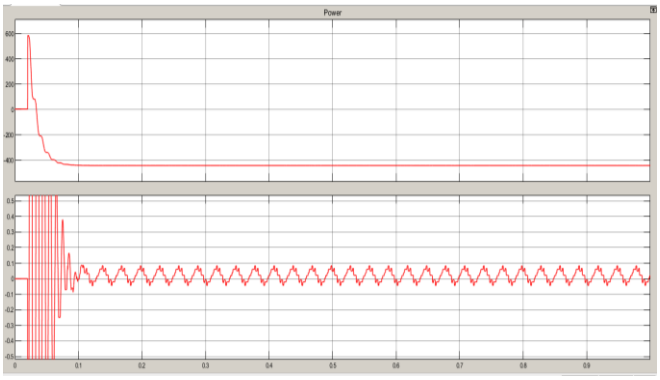

Figure 8: Grid Power Waveforms

Figures 9 load current and voltage waveforms the load current voltage observed is around 300 Volts and current is around 5 Amps.

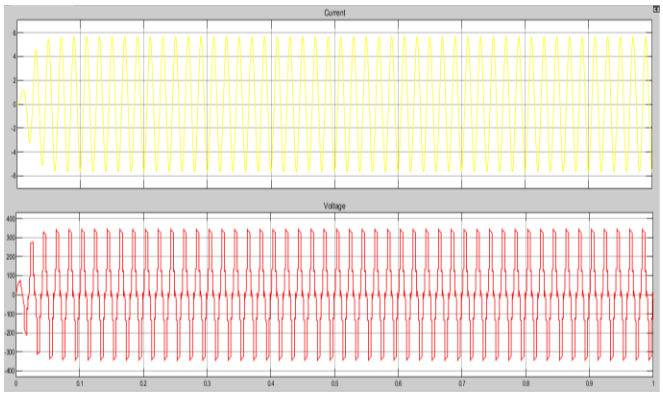

Figure 9: Load Current and Voltage Waveforms

The total harmonic distortion (THD) for the proposed circuit is found to be around 4.73%. Figure 10, shows the THD analysis.

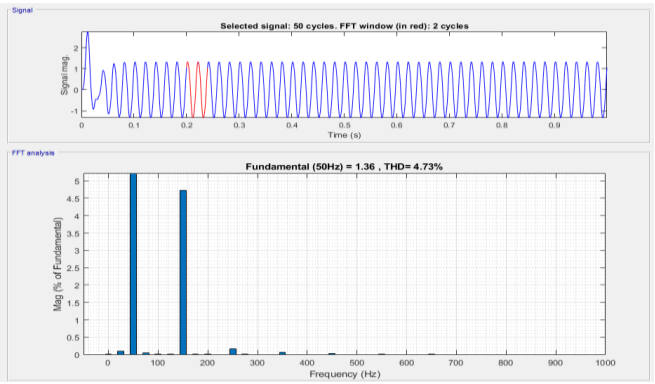

Figure 10: THD Analysis

7. CONCLUSION

A grid-connected solar power conversion system consisting of five levels, utilizing inverters, was suggested. Utilizing the fewest possible components for the five-level output, the new

topology is a modified H-bridge design. Operation of the IC-based MPPT maximizes the power extraction from the PV panels. A theoretical derivation and experimental validation are made about the efficient operation of the proposed H-bridge multilevel inverter. At roughly 4.74%, the THD. It also feeds back into the grid the PV power that remains after load power demand. Further improvements of the system are possible by using advanced MPPT algorithms such as Firefly, Most Valuable Player algorithm, etc for partial shading conditions.

REFERENCES

[1] S. K. Chattopadhyay and C. Chakraborty, ‘‘Full-bridge converter with naturally balanced modular cascaded H-bridge waveshapers for offshore HVDC transmission,’’ IEEE Trans. Sustain. Energy, vol. 11, no. 1, pp. 271–281, Jan. 2020, doi: 10.1109/TSTE.2018.2890575.

[2] A. Ahmed, M. S. Manoharan, and J.-H. Park, ‘‘An efficient single-sourced asymmetrical cascaded multilevel inverter with reduced leakage current suitable for single-stage PV systems,’’ IEEE Trans. Energy Convers., vol. 34, no. 1, pp. 211–220, Mar. 2019, doi: 10.1109/TEC.2018.2874076.

[3] X. Huang, K. Wang, B. Fan, Q. Yang, G. Li, D. Xie, and M. L. Crow, ‘‘Robust current control of grid-tied inverters for renewable energy integration under non-ideal grid conditions,’’ IEEE Trans. Sustain. Energy, vol. 11, no. 1, pp. 477–488, Jan. 2020, doi: 10.1109/TSTE.2019.2895601.

[4] G. Zhang, Z. Tian, P. Tricoli, S. Hillmansen, Y. Wang, and Z. Liu, ‘‘Inverter operating characteristics optimization for DC traction power supply systems,’’ IEEE Trans. Veh. Technol., vol. 68, no. 4, pp. 3400–3410, Apr. 2019, doi: 10.1109/TVT.2019.2899165.

[5] A. Kersten, O. Theliander, E. A. Grunditz, T. Thiringer, and M. Bongiorno, ‘‘Battery loss and stress mitigation in a cascaded Hbridge multilevel inverter for vehicle traction applications by filter capacitors,’’ IEEE Trans. Transport. Electrific., vol. 5, no. 3, pp. 659–671, Sep. 2019, doi: 10.1109/TTE.2019.2921852

[6] C. Liu, N. Gao, X. Cai, and R. Li, ‘‘Differentiation power control of modules in second-life battery energy storage system based on cascaded H-bridge converter,’’ IEEE Trans. Power Electron., vol. 35, no. 6, pp. 6609–6624, Jun. 2020, doi: 10.1109/TPEL.2019.2954577.

[7] S. Murshid and B. Singh, ‘‘Analysis and control of weak grid interfaced autonomous solar water pumping system for industrial and commercial applications,’’ IEEE Trans. Ind. Appl., vol. 55, no. 6, pp. 7207–7218, Nov. 2019, doi: 10.1109/TIA.2019.2939705.

[8] P. Omer, J. Kumar, and B. S. Surjan, ‘‘A review on reduced switch count multilevel inverter topologies,’’ IEEE Access, vol. 8, pp. 22281–22302, Jan. 2020, doi: 10.1109/ACCESS.2020.2969551.

[9] J. Ma, X. Wang, F. Blaabjerg, W. Song, S. Wang, and T. Liu, ‘‘Realtime calculation method for single-phase cascaded H-bridge inverters based on phase-shifted carrier pulsewidth modulation,’’ IEEE Trans. Power Electron., vol. 35, no. 1, pp. 977–987, Jan. 2020, doi: 10.1109/ TPEL.2019.2911422.

[10] J. Ma, X. Wang, F. Blaabjerg, W. Song, S. Wang, and T. Liu, ‘‘Multisampling method for single-phase grid-connected cascaded H-bridge inverters,’’ IEEE Trans. Ind. Electron., vol. 67, no. 10, pp. 8322–8334, Oct. 2020, doi: 10.1109/TIE.2019.2947864.

[11] Nirmal Mukundan C M, Vineeth K, Sooraj Suresh Kumar, Jayaprakash P, “Improved H-bridge Multilevel Inverter for Grid Integration of Photovoltaic Power Conversion System with Power Quality Enhancement”, 2020, IEEE International Conference on Power Electronics.

[12] M. S. B. Ranjana, P. S. Wankhade, and N. D. Gondhalekar, “A modified cascaded H-bridge multilevel inverter for solar applications,” 2014 Int. Conf. on Green Computing Comm. and Elect. Eng., Coimbatore, Mar 2014, pp. 17.

[13] Mr. Govind Metkar, Prof. Vaishali Malekar, “Design a Simulation of Multilevel Inverter for Reduction of Harmonics for Grid Connected PV System”, 2022, International Journal for Research in Applied Science & Engineering Technology (IJRASET).

[14] S. Mukherjee, “A SEPIC-Cuk-CSCCC Based SIMO Converter Design Using PSO-MPPT For Renewable Energy Application”, Journal of Electrical and Computer Engineering Innovations (JECEI), 2022.

[15] C. M. Nirmal Mukundan and P. Jayaprakash, “Solar PV fed cascaded Hbridge multilevel inverter and SIMO-SEPIC based MPPT controller for 3-phase grid connected system with power quality improvement,” 2017 Nat. Power Electron. Conf. (NPEC), Pune, Dec 2017, pp. 106-111.

[16] B. Xiao, L. Hang, J. Mei, C. Riley, L. M. Tolbert and B. Ozpineci “Modular Cascaded H-Bridge Multilevel PV Inverter With Distributed MPPT for Grid-Connected Applications,” IEEE Trans. on Ind. Apps., vol. 51, no. 2, Mar 2015 pp. 1722-1731.

[17] V. Sukanya, C. M. Nirmal Mukundan, P. Jayaprakash, O. V. Asokan “A new topology of multilevel inverter with reduced number of switches and increased efficiency,”

2018 IEEE Int Conf on Power Electronics Drives and Energy Systems (PEDES), Dec 2018, pp. 1-6.

[18] Xiao. W., Ozog. N., Dunford. W. G., "Topology study of PV interface for maximum power point tracking," IEEE Trans. Ind. Electron., Apr 2007, 54,(3), pp. 1696-1704.

[19] Roberto Gonzlez, Eugenio Guba, Jess Lpez and Luis Marroyo, "Transformerless Single-Phase Multilevel-Based PV Inverter," IEEE Tran. on Ind. Electron., vol. 55, no. 7, July 2008, pp. 2694-2702.

[20] H. Vahedi, M. Sharifzadeh and K. Al-Haddad, "Modified Seven-Level Packed U-Cell Inverter for Photovoltaic Applications," IEEE Jour. of Emerg. & Selected Topics in Power Electron., vol. 6, no. 3, Sept 2018 pp. 1508-1516.

[21] Hani Vahedi, P. A. Labb and K. Al-Haddad, "Sensor-Less Five-Level Packed U-Cell (PUC) Inverter Operating in Stand-Alone and GridConnected Modes," IEEE Tran. on Ind. Info., vol. 12, no. 1, Feb 2016 pp. 361-370.

[22] Marco di Benedetto, A. Lidozzi, F. Crescimbini and P. J. Grbovic, "Five Level E-Type Inverter for Grid-Connected Applications," IEEE Tran. on Ind. Ap., vol. 54, no. 5, Sept. 2018 pp. 5536-5548.